SPACE STATION STRUCTURAL DYNAMICS/ REACTION CONTROL SYSTEM INTERACTION STUDY

M. Pinnamaneni [1] and J. Murray [2]

Martin Marietta Denver Aerospace, Denver, Colorado

Abstract

The performance of the Reaction Control System is impacted by the extreme flexibility of the space station structure. This paper [3] presents the method used to analyse the periodic thrust profile of a simple form of phase plane logic. The results illustrate the effect on flexible body response of 1) the type of phase plane logic utilized and 2) the choice of control parameters: cycle period and attitude deadband.

1. Staff Engineer, Analytical Mechanics. Member AIAA.
2. Staff Engineer, Guidance Navigation and Control. Member AIAA.
3. Sponsored by Martin Marietta Corporation, Independent Research and Development, D37S.

Glossary

a'_n	=	Fourier coefficient, normalized by the control torque
A	=	complex harmonic response
		suffix R: real component
		suffix I: imaginary component
$\Delta P'$	=	thrust pulse, normalized by P
Δt	=	cycle period fraction
		suffix 1: control phase
		suffix 2: coast phase
ε	=	attitude error angle
		suffix DB: deadband half-angle
$\dot{\varepsilon}$	=	error angle rate
		suffix MAX: maximum
		suffix H: hard-cycle
f_C	=	duty cycle
f	=	frequency (Hz)
		suffix S: structural
		suffix H: harmonic
F	=	thrust profile harmonic coefficient
H	=	transfer function
I	=	inertia
L	=	propulsion efficiency losses
		suffix F: thrust losses
		suffix I: impulse losses
ϕ	=	attitude angle
n	=	Fourier harmonic
		suffix PEAK: corresponding to a peak
P	=	cycle period
		suffix S: soft-cycle
		suffix SC: coast
		suffix C: hard-cycle
$\Sigma\phi$	=	attitude deadband
t	=	time
T	=	applied torque
T'	=	angular acceleration
		suffix C: control
		suffix D: disturbance

1. INTRODUCTION

Due to the extreme mechanical flexibility of the space station, the use of thrusters to control attitude presents new challenges to control system designers. The lightweight materials being used to construct the space station effect low rigidity and low natural damping. This, in turn, causes the presence of a large number of low frequency structural modes which place stringent limits on the control system bandwidth. The objective of this paper is to describe an approach to designing the control algorithm via analysis of the flexible body response to thrust profiles.

There is a very practical reason for this approach: as thrust profile requirements become more exacting and sophisticated, the propulsion system life cycle costs can become prohibitive. It is therefore expedient to analyse the interaction between thruster control and structural dynamics in order to affect thruster attitude control requirements that are cost effective.

The analysis covers two operational scenarios: space station reboost and back-up control during failure of the primary Attitude Control System (ACS). In each case the goal is to keep the attitude error within a 10 degree band, although minimizing the thrust cosine losses during reboost is also considered. (The essential difference between the two is the size of the disturbing torque seen by the space station, the reboost disturbance is significantly larger). The same phase plane logic has been used to generate thrust profiles for both scenarios. Based on attitude error and error rate, it has been used in other systems where structural modes are easily excited. As will be shown, thrust profile demands can be generated which restrict the harmonic content responsible for exciting the structure.

The approach to the dynamic analysis is to first analyse the space station rigid body response to the thrust profiles generated by the phase plane logic. These profiles are periodic and can be stipulated based on attitude control requirements and space station inertias, the shape of the thrust profile will vary according to the size of the disturbing torque and control torque.With the variation in shape determined, the Fourier coefficients are calculated showing the harmonic content of each profile. This enables a first cut at establishing the profile period.

A structural dynamic model is used during the second stage of the analysis, based upon the MMA Twin Keel configuration (dated 1/15/86.) The frequency response to thrust pulses is determined at various locations on the station to identify the significant elastic modes which might influence the phase plane logic design, and also establish a lower bound to the profile period. The final step is to define thrust profiles which restrict structural response and compute the actual response from model results.

This paper provides an insight into the development of Reaction Control System (RCS) requirements by analysing the sensitivety of thrust profiles to attitude control requirements and space station flexibility. It also illustrates how a relatively simple control algorithm can effect a 2 degree attitude band during the space station reboost and ACS backup.

2. PHASE PLANE LOGIC THRUST PROFILES

2.1 PHASE PLANE ROTATION

Introduction

The approach taken to develop the phase plane logic is to allow the space station to "float" within a deadband. Torques are applied only to reverse the direction of rotation when an attitude error limit has been reached. This is illustrated in Figure 2.1.

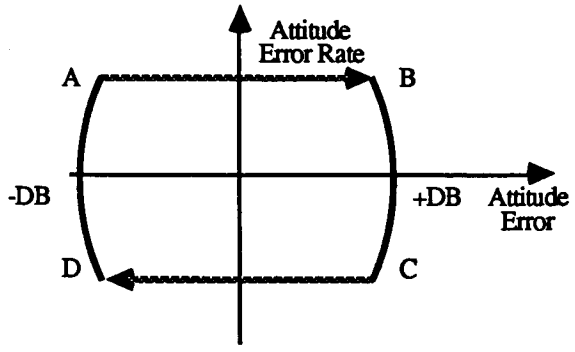

Fig. 2.1 Phase Plane Limit Cycle

As can be seen, the space station is allowed to float from one side of the dead band to the other (A to B and C to D). Control torques are applied when the space station attitude reaches the deadband (B to C and D to A).

This kind of limit cycle is referred to as hard due to there being two torque impulses for each cycle. In comparison, a soft limit cycle utilizes disturbance torques such that only one torque impulse is required to complete a cycle[1]. This is illustrated in Figure 2.2.

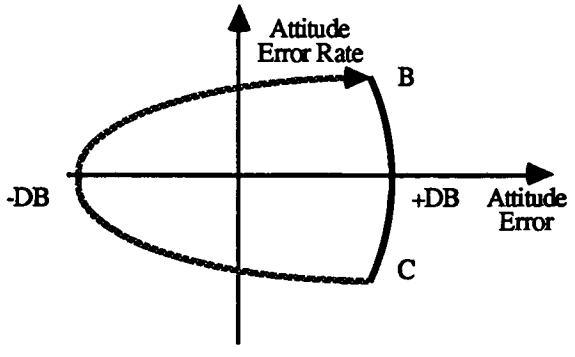

Fig. 2.2 Soft Limit Cycle

As shown, only one torque pulse is required for each cycle (B to C). The disturbance torque acts to rotate the space station back (C to B).

Rigid Body Rotational Equations of Motion

The set of rigid body equations for a single rotation axis can be described by the following equations:

$$\ddot{\phi} = T' \qquad \text{____ 2.1}$$

$$\dot{\phi}(t) = T'.[t-t_0] + \phi(t_0) \qquad \text{____ 2.2}$$

$$\phi(t) = T'.[t-t_0]^2/2 + \dot{\phi}(t_0).[t-t_0] + \phi(t_0) \qquad \text{____ 2.3}$$

where:

$T' = T/I$

T = applied torque, assumed constant

I = space station inertia

t_0 = initial time

$\phi(t_0)$ = initial attitude angle

Cycle Period of a Soft Limit Cycle

The soft-cycle period is the sum of the torque impulse period, Δt_1, and the soft-cycle coast period, Δt_2. Equation 2.2 yields the torque impulse period:

$$\Delta t_1 = 2.\dot{\varepsilon}_{MAX} / T'_C \qquad \text{____ 2.4}$$

where:

$\dot{\varepsilon}_{MAX}$ = maximum soft-cycle error rate

T'_C = control angular acceleration

The soft-cycle coast period, Δt_2, is calculated from equation 2.2 and 2.3 assuming a constant disturbance torque, T'_D. Hence:

$$\Delta t_2 = 8.\varepsilon_{DB}/\dot{\varepsilon}_{MAX} \qquad \text{____ 2.5}$$

$$\dot{\varepsilon}_{MAX}^2 = 4.(T'_D.\varepsilon_{DB}) \qquad \text{____ 2.6}$$

where:

ε_{DB} = attitude deadband half-angle

T'_D = disturbance angular acceleration

The soft-cycle can be summarized by:

$$P_S = P_{SC}.\{ 1 + T'_D/T'_C \} \qquad \text{____ 2.7}$$

where:

$$P_{SC} = 4.\{\varepsilon_{DB}/T'_D\}^{1/2} \qquad \text{____ 2}$$

Comparison of Hard and Soft Limit Cycles

Because the hard limit cycle has no disturbance torque, the cycle period is simply computed from:

$$P_C = 2.\{2.\dot{\varepsilon}_H/T'_C + 2.\varepsilon_{DB}/\dot{\varepsilon}_H\} \quad \text{____ 2.9}$$

where: $\dot{\varepsilon}_H$ = equivelant hard-cycle error rate

From equations 2.8 and 2.9 an equivalent hard-cycle error rate can be related to the maximum soft-cycle error rate for identical periods and deadbands. This yields:

$$\dot{\varepsilon}_H = \dot{\varepsilon}_{MAX}/2 \quad \text{____ 2.10}$$

As can be seen, the resultant change in angular velocity over a complete cycle is the same. Consequently, the torque impulse is also identical, as illustrated in Figure 2.3.

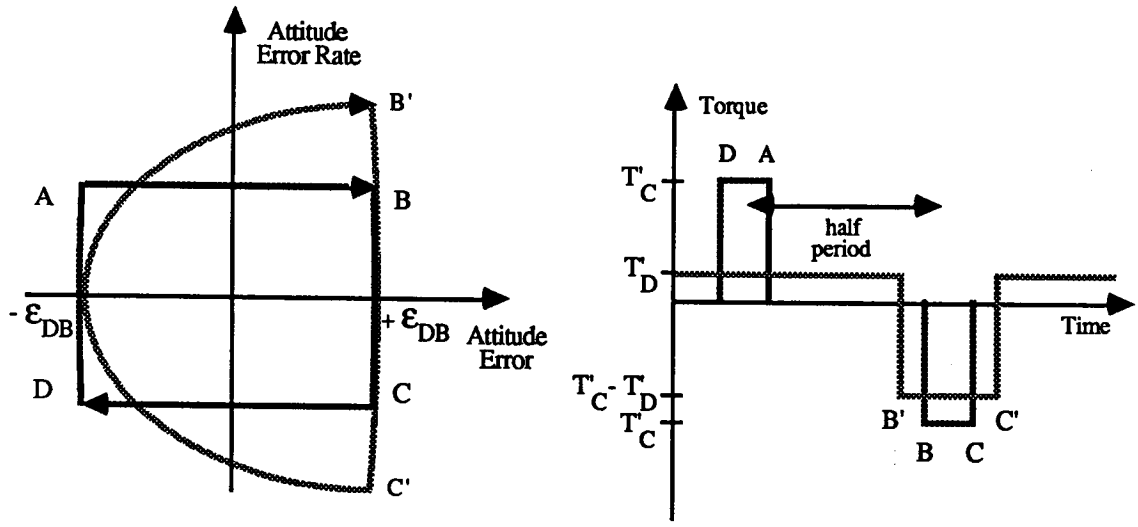

Figure 2.3 Phase Plane and Torque Profile Comparison

Space Station utilization of the Soft Limit Cycle

During reboost, the space station thrust axis is sufficiently displaced off the CG to cause a large disturbance torque and, as a result, the hard-cycle phase plane logic is not feasible. Given a fixed deadband and a knowledge of the disturbance torque, the torque profile can be shaped to effect the largest practicle cycle period. This minimizes the thruster harmonics as will be shown.

Should the RCS be used to backup an ACS failure, the disturbance torque (a function of the gravity gradient and aerodynamic torques) is small. The soft-cycle is still the optimum solution as long as the torque requirement (B' to C') does not effect a thrust impulse less than the minimum impulse bit. In comparison to the reboost case, the same deadband will effect a longer cycle period (ref. equation 2.8) further reduces the thruster harmonics.

2.2 THRUST IMPULSE LOSSES

Calculating the losses

During reboost the thrust vector is rotating about about the velocity vector as the space station attitude rotates about the deadband. This effects a reduction in effective impulse due to cosine losses. The fractional thrust loss can be calculated from:

$$L_F(t) = 1 - \cos \varepsilon(t) \qquad \text{____ 2.11}$$

and the fractional impulse loss over half of the coast period:

$$L_I = 1/\Delta t \int_0^{\Delta t} [\, 1 - \cos \varepsilon(t) \,] \, . \, dt \qquad \text{____ 2.12}$$

For the hard limit cycle we have:

$$\Delta t = 2.\varepsilon_{DB}/\dot{\varepsilon}_H$$

and $$\varepsilon(t) = \varepsilon_{DB} - \dot{\varepsilon}_H.t \qquad \text{____ 2.13}$$

substituting into 2.12 we have:

$$L_I = \{ \cos \phi_{DB}/2 \, . \, \sin \phi_{DB} - \sin \phi_{DB}/2 \, . \, (\cos \phi_{DB} - 1) \} / \phi_{DB} \qquad \text{____ 2.14}$$

where: $$\phi_{DB} = 2.\varepsilon_{DB}$$

For the soft-limit cycle the integral is evaluated after substituting equations 2.3 and 2.6:

$$L_I = 2/\Delta t \int_0^{\Delta t_2/2} \{1 - \cos [(a.t - b)^2 - \varepsilon_{DB}]\} \, dt \qquad \text{____ 2.15}$$

where: $$a = \{T_D / 2\}^{1/2}$$

$$b = \phi_{DB}$$

Integrating 2.15 we have:

$$L_I = 1 - \cos \phi_{DB}/2 \, . \, \Sigma\{(-1)^n \, . \, \phi_{DB}{}^{2n} / [(4n+1).(2n)!]\} - \sin \phi_{DB}/2 \, . \, \Sigma\{ (-1)^n \, . \, \phi_{DB}{}^{2n+1} / [(4n+3).(2n+1)!]\} \qquad \text{____ 2.16}$$

Estimating the Losses

For small deadbands a simplifying approximation, $\phi_{DB}=\sin \phi_{DB}$, can be made to equations 2.14 and 2.15:

$$L_{I(HC)} = 1 - (\cos \varepsilon_{DB} + \varepsilon_{DB}^2)$$

and

$$L_{I(SC)} = 1 - (\cos \varepsilon_{DB} + 2.\varepsilon_{DB}^2/3) \qquad \text{2.17}$$

As can be seen, the two limit-cycle types have nearly identical impulse loss characteristics. The actual losses described by equations 2.14 and 2.16 are illustrated in Figure 2.4. In both cases the impulse loss is relatively insensitive to the deadband size, with a 25 degree deadband the impulse loss is little more than 1%. It can be concluded that impulse loss is not a descriminator.

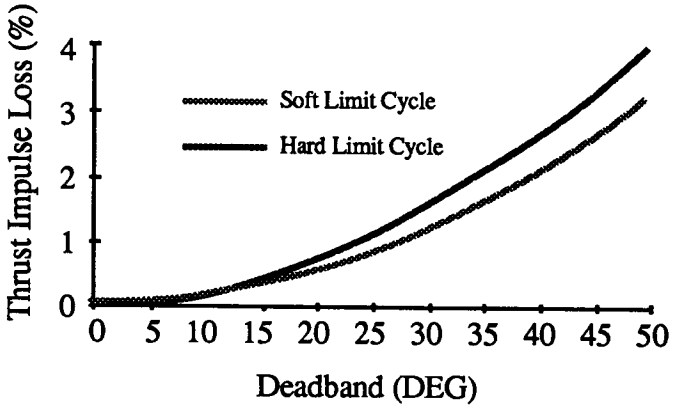

Figure 2.4 Estimate of Thrust Impulse Losses

2.3 SOFT LIMIT CYCLE PERIODS AND DUTY CYCLE

Duty Cycle

Figure 2.5 illustrates a worst case reboost thrust off-set in the space station pitch plane. This off-set is the effect of the bottom set of propulsion modules being further displaced from the space station CG than the top set.

The disturbance-control torque ratio can be calculated as follows:

$$T_C = F * 6.5 \text{ bays}$$

$$T_D = 2.F * 1 \text{ bay}$$

Hence

$$T'_D/T'_C = 0.31 \qquad \text{2.18}$$

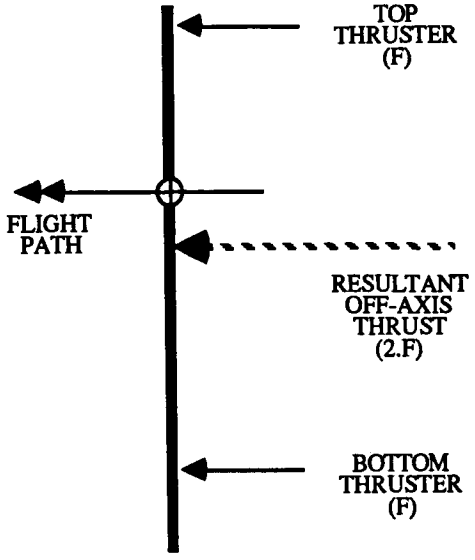

Figure 2.5 Space Station Thrust Misalignment during Reboost

The duty cycle required to effect a pitch control is calculated using a rearrangement of equation 2.7:

$$f_C = [P_S - P_{SC}] / P_S$$

$$= [T'_D / T'_C] / [1 + T'_D / T'_C] \qquad \text{2.19}$$

where f_C = duty cycle

This is illustrated in Figure 2.6 for a torque ratio range (0,0.3).

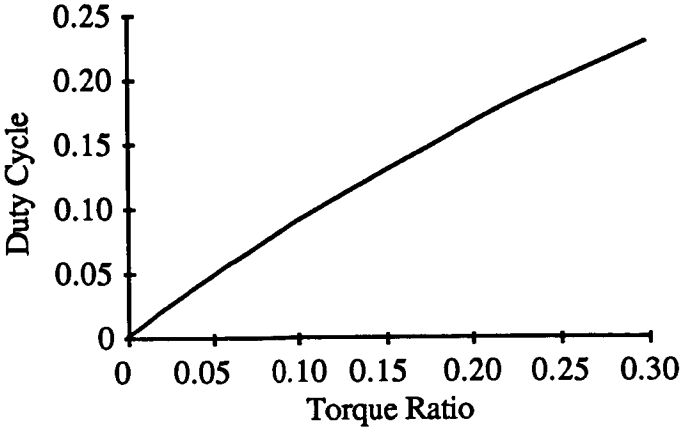

Figure 2.6 Duty Cycle vs Torque Ratio

In comparison to the reboost case, during ACS backup the disturbance due to gravity gradient and aerodynamic torques are small, in the region of 20 to 40 Nm. The range of available control torques depends on the final thruster size and the control mode: top thruster only, bottom thruster only or both sets of thrusters to provide a couplet. The impact of these possibilities on the torque ratio is illustrated in Table 2.1.

	Top Thruster Set	Bottom Thruster Set	Combined Thruster Set
Control Torque Range (Nm)	2,400-6,000	4,000-10,000	6,400-16,000
Torque Ratio Range (40N thruster)	0.008-0.016	0.005-0.010	0.003-0.006
Torque Ratio Range (100N thruster)	0.003-0.006	0.002-0.004	0.001-0.005

Table 2.1 Torque Ratio Variation with Thruster Size and Usage

As can be seen, the thruster duty cycle during the ACS backup mode are two orders less than those of the reboost mode. There are two critical parameters related to the duty cycle: the minimum impulse bit and thruster heat pumping. Assuming a 60 second limit cycle period, the required minimum impulse is in the 60 to 100 msec range which should not impact the design. The second parameter concerns thruster heat pumping; this is where the fuel flow is insufficient to cool the thruster due to its being discontinuous. Figure 2.7 illustrates this phenomenon for a typical hydrazine application showing the operating modes for both the reboost and ACS backup modes. The ACS backup mode presents the most severe operating condition. However, because this mode is abnormal it cannot be assumed that it will effect either design or life cycle difficulties.

Cycle Period

The cycle period determines the thruster harmonics exciting the structure. It is therefore desirable to maximize the cycle period to the extent possible in order to minimize the magnitude of the higher frequency harmonics. This is acheived by increasing the deadband.

The attitude control deadband has two components, illustrated in Figure 2.8: the error angle (ε_{DB}) seen during the coast phase of the cycle, and the control error angle (ϕ'_{DB}) seen during the control phase of the cycle. Equations 2.7 and 2.8 define the cycle period as a function of the error angle and the torque ratio, the deadband is determined a follows:

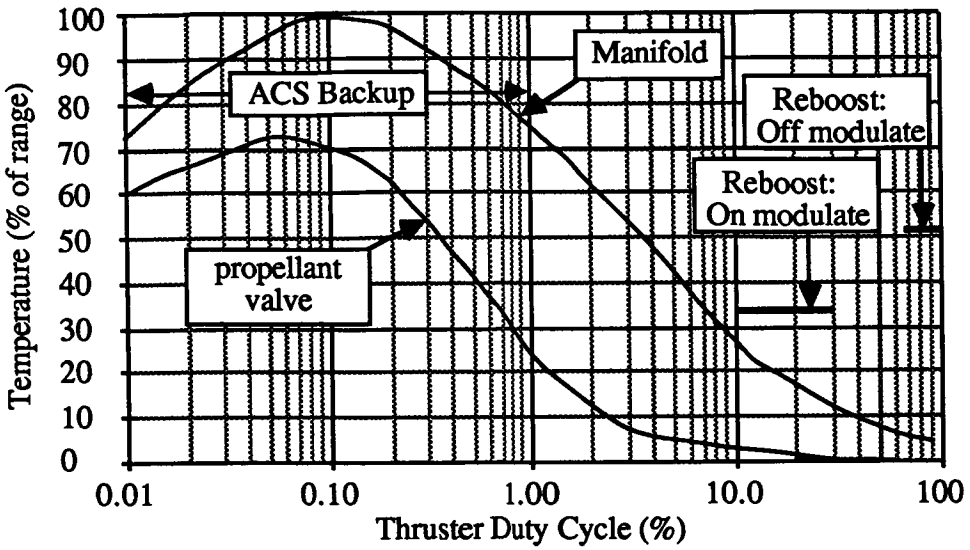

Figure 2.7 Heat Pumping vs Duty Cycle

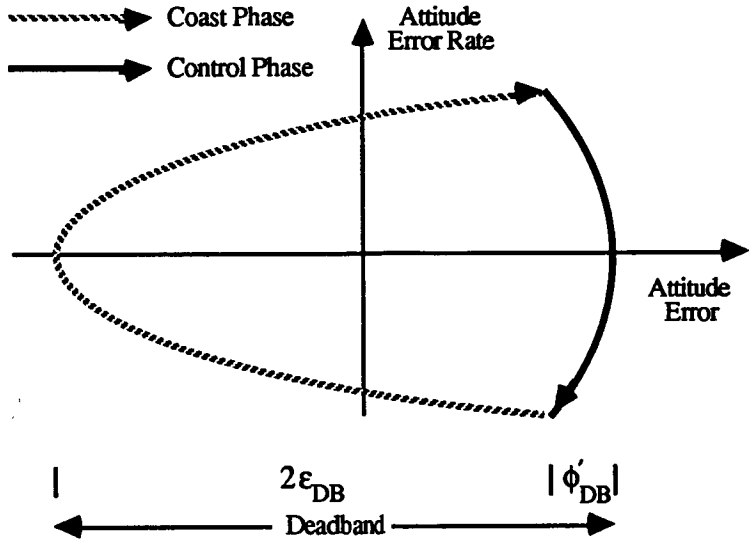

Figure 2.8 Soft Limit Cycle Deadband

From equation 2.3 we have:

$$\phi'_{DB} = [T_C/2].(\Delta t_1/2)^2 + \dot{\varepsilon}_{MAX}.(\Delta t_1/2) \quad \text{____ 2.20}$$

and, $$\dot{\varepsilon}_{MAX} = T'_C.\Delta t_1/2$$

therefore, $$\phi'_{DB} = 3.\dot{\varepsilon}_{MAX}^2 / (2.T'_C) \quad \text{____ 2.21}$$

Substituting in equation 2.6 we have:

$$\phi'_{DB} = [T'_D/T'_C].6.\varepsilon_{DB} \quad \text{____ 2.22}$$

The error angle can now be defined as a function of the total deadband, $\Sigma\phi$:

$$\varepsilon_{DB} = \Sigma\phi /\{ 2.(1 + 3.[T'_D/T'_C]) \} \quad \text{____ 2.23}$$

From equations 2.7, 2.8 and 2.23 the soft-cycle period can be plotted against the total deadband as illustrated in Figure 2.9. A comparison of 30% and 0.1% torque ratio is given in Figure 2.10.

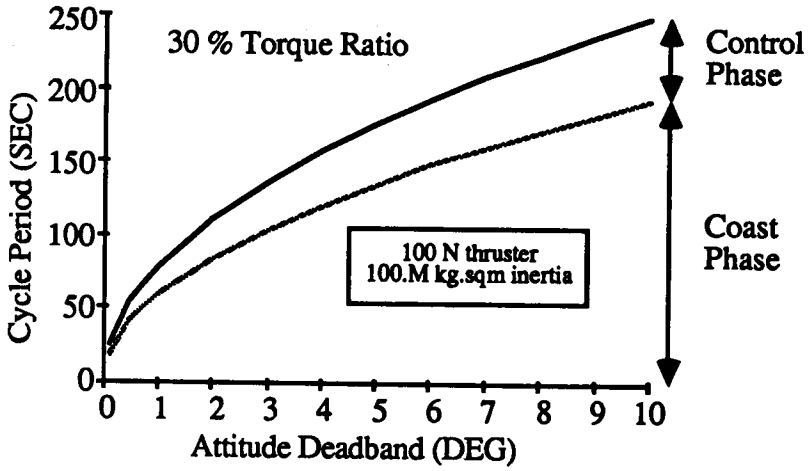

Figure 2.9 Variation of Cycle Period with Attitude Deadband

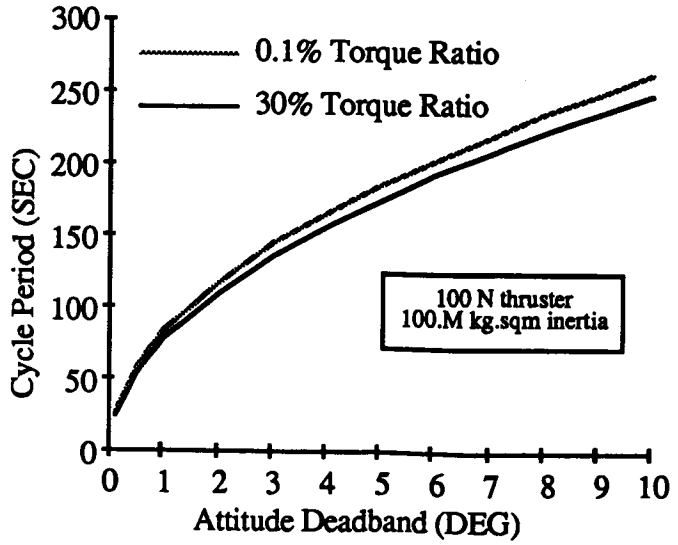

Figure 2.10 Variation of Cycle Period with Torque Ratio

From Figures 2.9 and 2.10 it can be seen that the cycle period is sensitive to the attitude deadband. The configuration used to generate these characteristics is a worse case as 100N thrusters were modelled; 40N thrusters would increase the period by 60%, and during the ACS backup mode the period would be increased ten-fold.

It can be concluded that a period range of 60 to 240 seconds for the space station is quite feasible with an attitude deadband during ACS backup within 2 degrees.

2.4 PRELIMINARY CONCLUSIONS

Reboost Mode

It has been shown that a soft limit cycle can be implemented to effect attitude control. This requires on-off modulation of the thrusters; either off-modulating thrusters with the largest moment arm at a 20% rate (80% duty cycle), or on-modulating the redundant thrusters having the smallest moment arm at a 20% rate (20% duty cycle). The remainder of this study will consider the latter as a worst case scenario.

The attitude deadband is largely insensitive to impulse losses and mostly dependent upon the required cycle period. Periods of 60 to 240 seconds in the pitch plane are quite feasible using deadbands of 1 to 10 degrees. An analysis of the structural response to thruster harmonics is required to determine the sensitivity to cycle period.

ACS Backup Mode

It has been shown that a soft limit cycle is equally effective during ACS backup. Although the duty cycle is significantly smaller than that of the reboost mode, the minimum impulse requirement is still significantly larger than the minimum impulse bit (2 seconds as compared to 40 msecs.) A more significant problem may be the heat pump phenomenon at the low duty cycle rate experienced. However, given that this mode is abnormal it is not considered to be a serious handicap.

3.LIMIT CYCLE HARMONICS

3.1 SOFT LIMIT CYCLE

Analysis of the thruster induced harmonics provides insight into the space station structural excitation. To determine the affect of the soft limit cycle, the torque profile illustrated in Figure 2.3 is used to calculate the Fourier coefficients as follows:

$$a_0 = [1/P].\int_{-P/2}^{P/2} [T'_D + T'_C(t)].dt$$

$$a_n = [2/P].\int_{-P/2}^{P/2} [T'_D + T'_C(t)].\cos n\omega t.dt$$

$$b_n = [2/P].\int_{-P/2}^{P/2} [T'_D + T'_C(t)].\sin n\omega t.dt \qquad \text{____ 3.1}$$

Since the function has even symmetry, $b_n = 0$. Also, by definition the integral of torque over the cycle period is zero, therefore $a_0 = 0$. The Fourier coefficient (normalized by the control torque) is:

$$a'_n = [2/n\pi].\sin (n.\Delta P'.\pi) \qquad \text{____ 3.2}$$

where: $\Delta P'$ = thrust pulse duration, normalized by the cycle period.

The frequency spectrum of T'_C is illustrated in Figure 3.1 for a 20% pulse duration (note that for a soft limit cycle the pulse duration is analogous to the duty cycle.)

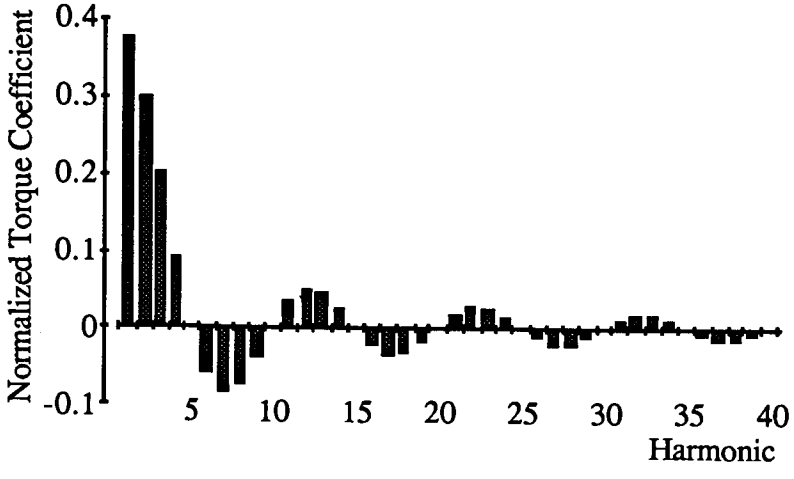

Figure 3.1 Soft Limit Cycle Frequency Spectrum

The significance of this spectrum lies in recognizing the fast decay in the size of the higher frequency harmonics. The correct choice for cycle period will effectively restrict the size of the harmonics that excite the space station structural modes. The cycle period can be set using:

$$P_S > n / f_M \qquad \text{____ 3.3}$$

For example; if the structural mode of concern has a 0.1 Hz frequency and the 10th harmonic is considered the breakpoint, then the cycle period must exceed 100 seconds. The detailed analysis of this control-dynamics interaction is the subject of section 5 of this paper.

3.2 COMPARISON OF HARD AND SOFT CYCLE HARMONICS

The derivation of Fourier coefficients for the eqivelent hard limit cycle is identical to that of the soft. For the torque profile illustrated in Figure 2.3, the coefficients can be calculated using:

$$a'_n = [2/n\pi].\{\sin(n.\Delta P'.\pi/2) + (-1)^n.\sin(n.\Delta P'.\pi/2)\} \quad \text{3.4}$$

Figure 3.2 compares the two cycle types illustrating two principle differences:

a. The decay of the hard limit cycle harmonics is slower than that of the soft limit cycle.

b. The hard limit cycle has less harmonics. (Although in reality the space station would not have the identical opposing torque impulses used to derive the results given in Figure 3.2, consequently there would not be the exact cancellation shown here.)

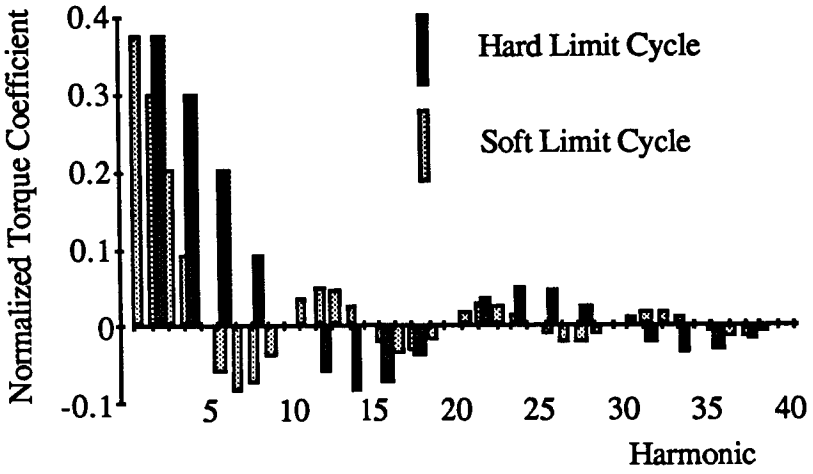

Figure 3.2 Comparison of Hard and Soft Limit Cycle Frequency Spectrums

To effect a separation of torque profile harmonics and structural modes identical to that of the soft limit cycle would require a period twice the size. This can be seen from the comparison in Figure 3.2; the 20th harmonic of the hard-cycle is equivelent to the 10th harmonic of the soft-cycle with respect to the magnitude of the torque coefficients. It should be noted, however, that a complete dynamic response analysis is necessary to validate this assertion.

3.3 EFFECT OF COEFFICIENT DECAY ON DYNAMIC RESPONSE

Peak Torque Decay in the Frequency Domain

The amplitude of the peak torque Fourier coefficients can be determined from equation 3.2:

$$A_P = 2.T_C / n.\pi \quad \text{____ 3.5}$$

Substituting the harmonic, n, with frequency and expressing in db, the variation of peak amplitude with frequency as described by:

$$20 \log A_P = 20 \log[\, 2.T_C/\pi.\Delta P/P \,] - 20 \log[\, \Delta P.f \,] \quad \text{____ 3.6}$$

This is described graphically in Figure 3.3:

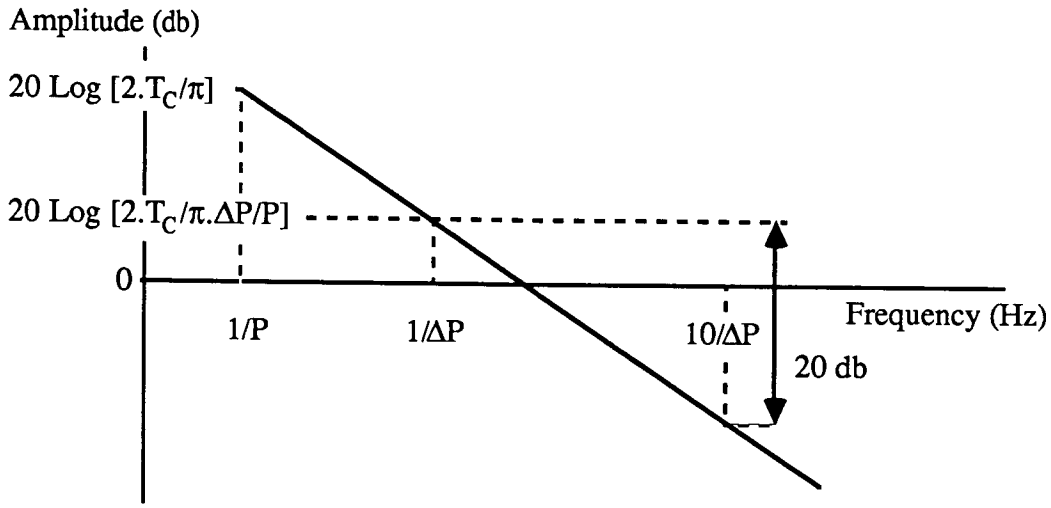

Figure 3.3 Decay of Peak Disturbance with Frequency

As can be seen the peak amplitudes decay at a 20db/decade rate. There are three significant parameters that will determine the eventual frequency response: the control torque, duty cycle and the thruster pulse width. From equation 2.19, the following simplification can be made to equation 3.6:

$$20 \log A_P = 20 \log[\, 2.T_D/\pi \,] - 20 \log[\, P.(T'_D/T'_C).f \,] \quad \text{____ 3.7}$$

From equation 3.7 it is more evident that the driving parameters are the disturbance torque, the cycle period and the torque ratio. Hence, recalling Figure 2.9, it can be seen that constraining the high frequency content of the thrust profile requires decreasing the size of the disturbance torque and increasing the deadband.

Effect of Peak Torque Decay on Flexible Body Response

The need to restrict the high frequency content of the thruster profile becomes evident when the flexible body response is assessed. This is illustrated qualitatively in Figure 3.4 as two

predominant flexible body modes, the second larger than the first (note that in reality there will tend to be alot more than two!)

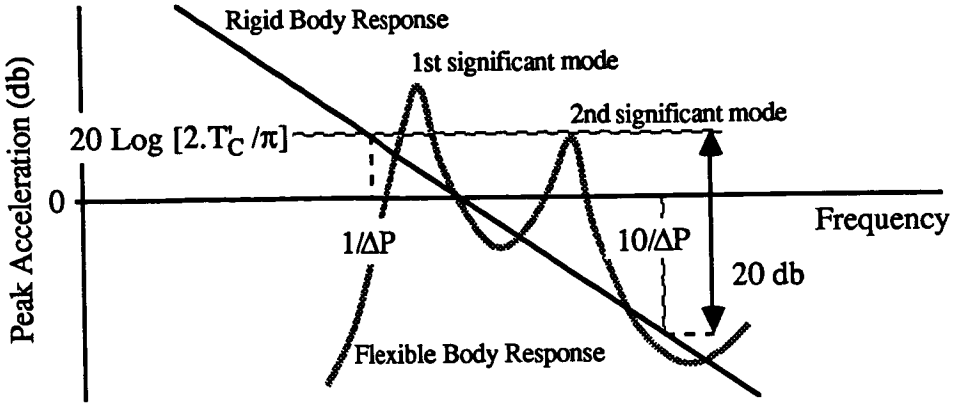

Figure 3.4 Flexible Body Response

Figure 3.4 illustrates the rigid body response, with the flexible body response superimposed. As the thruster pulse width is reduced, the response of both modes will increase. Also, because the exciting torque has a -20db/decade slope, the second mode has a smaller response even though it is more "excitable".

4. FLEXIBLE BODY DYNAMIC RESPONSE ANALYSIS

4.1 STRUCTURAL DYNAMIC MODEL.

In order to analyse the RCS-Structural dynamics interaction, a finite element model has been developed based on the Martin Marietta Space Station dual keel 5 meter configuration (dated 1/15/86). The truss members were modelled with ROD elements and the solar panels, radiators and modules were assumed rigid and modelled with mass elements at the corresponding interfaces neglecting the moment of inertias. These simplifications eliminate the very low frequency local modes and provide the primary modes necessary for the RCS/Structural Dynamics interaction study. The mass properties of the finite element model illustrated in Figure 4.1 are described in the Table 4.1. The size of the finite element model (1596 d.o.f) was reduced to a smaller dynamic model (42 d.o.f) using MSC/NASTRAN generalised dynamic reduction procedure. The reduced model has the fidelity of generating natural frequencies accurately up to 2.0 Hz.

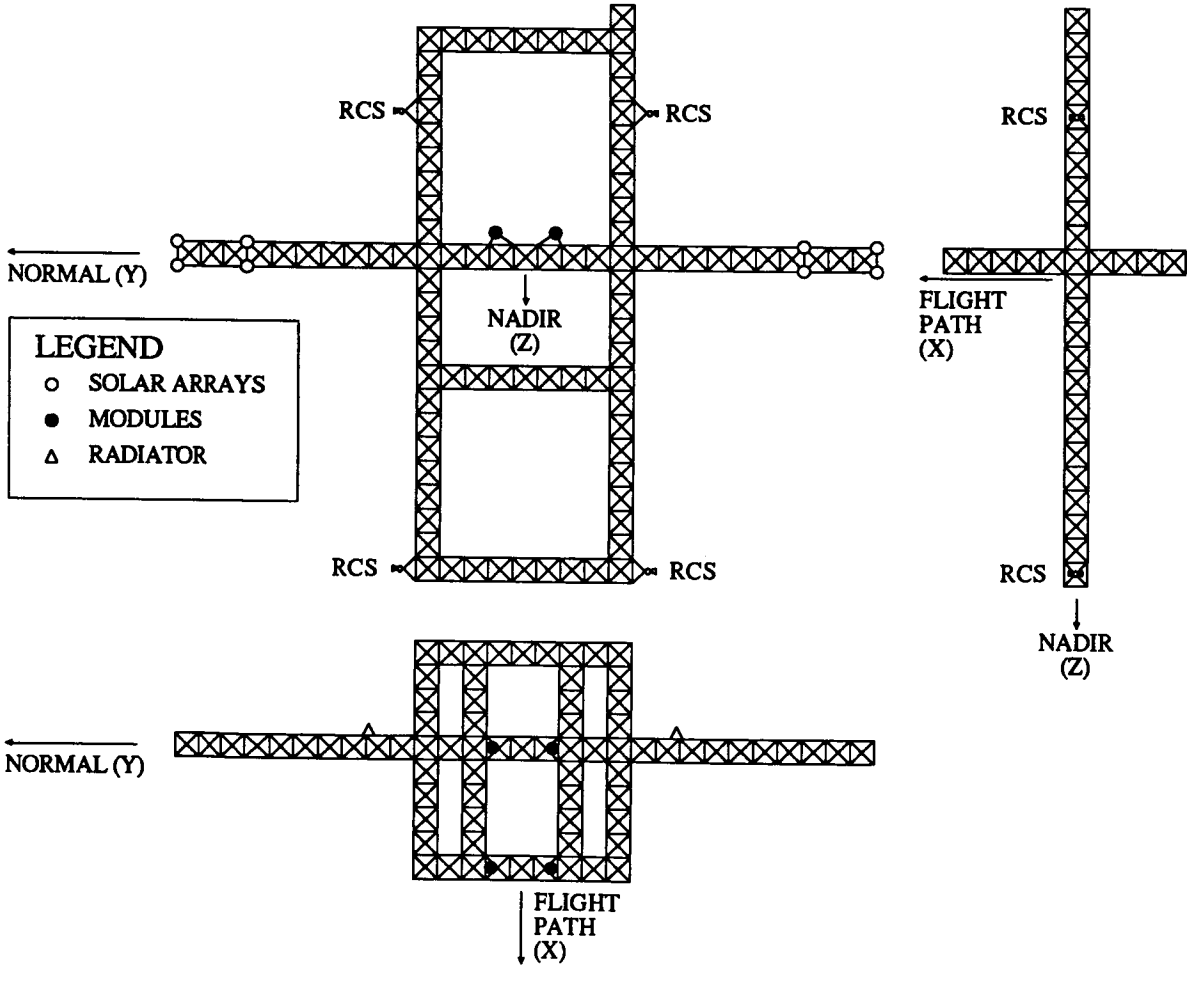

Figure 4.1 Martin Marietta Space Station Dual Keel 5m Configuration NASTRAN Model

Mass (kg)	217,404		
Centre of Gravity	X 5.316	Y -0.248	Z -3.513
Inertia (kg.m^2)	I_{XX} $1.08*10^8$	I_{YY} $8.71*10^7$	I_{ZZ} $7.75*10^7$
Inertia (kg.m^2)	I_{XY} $2.17*10^6$	I_{XZ} $2.36*10^6$	I_{YZ} $4.59*10^6$

Table 4.1 MMA Dual Keel 5m Space Station Configuration Mass Properties

4.2 NORMAL MODES.

MSC/NASTRAN SOL 3 was used to obtain the natural frequencies and mode-shapes up to 2.0 Hz. The frequencies of the elastic modes are listed in the Table 4.2 along with the modal strain and kinetic energy participations of the different structural components. These energy participations provide insight into identifying the most significant modes that make up the dynamic response. For example, the thruster located on the top keel in the flight direction (X-axis) significantly excites the 0.36 Hz and 0.54 Hz elastic modes. Similarly, the thruster located on the bottom keel excites the 0.42 Hz, 0.94 Hz and 1.17 Hz modes. Since the present study considers only the thruster on the top keel, the 0.36 and 0.54 elastic mode-shapes are presented in the Figures 4.2 and 4.3 .

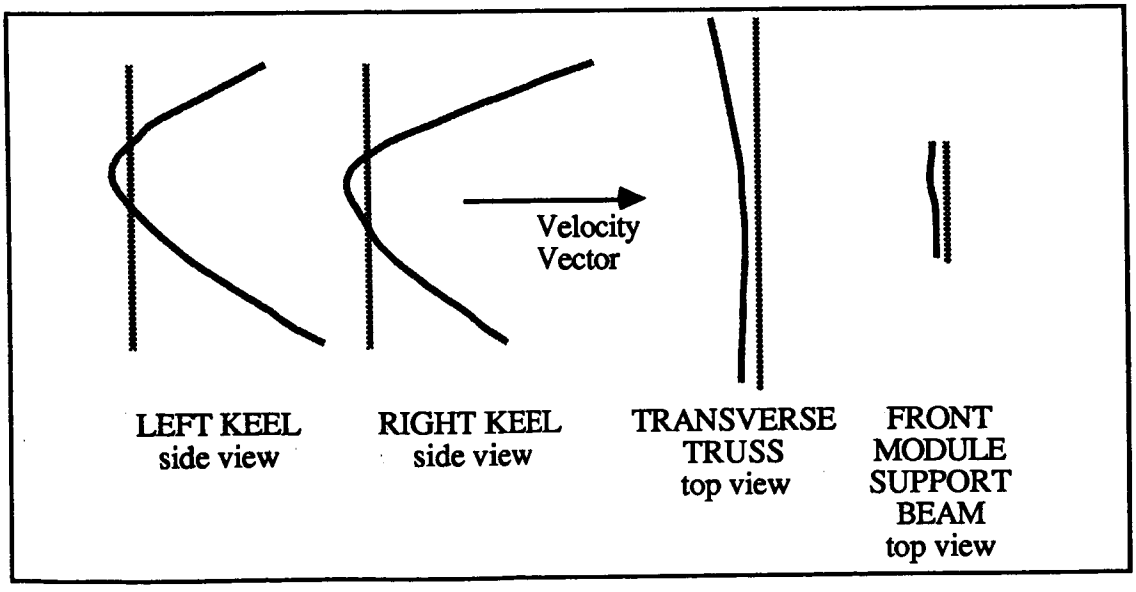

Figure 4.2 Mode-Shape deflections at 0.36 Hz

Freq (Hz)	Model Percentage Strain-Kinetic Energy							Mode and Mode Description
	1	2	3	4	5	6	7	
0.36	2-1	2-1	62-60	8-14	21-6	3-17	2-1	1. UPPER KEEL FIRST X BENDING (SYM)
0.42	4-2	4-2	2-2	40-49	43-41	5-2	3-2	2. LOWER KEEL FIRST X BENDING (SYM)
0.53	27-47	26-42	5-2	4-1	34-6	2-1	2-1	3. TRANSVERSE BOOM FIRST Z BENDING
0.54	5-1	5-2	56-77	7-5	13-13	11-1	7-1	4. UPPER KEEL FIRST TORSION, BEND, PITCH
0.56	24-46	25-46	2-1	2-1	37-4	5-1	5-1	5. TRANSVERSE BOOM FIRST X BENDING
0.57	3-25	3-15	48-52	2-1	18-5	3-1	3-1	6. UPPER KEEL Y , TRANSVERSE X BENDING
0.62	26-28	25-44	3-1	4-10	28-15	7-1	7-1	7. TRANSVERSE BOOM X & Z BENDING
0.67	19-26	20-16	16-13	8-18	27-23	4-1	3-3	8. UPPER KEEL Y, TRANSVERSE X & Z BEND
0.91	8-2	8-2	11-7	54-62	10-22	5-2	4-2	9. LOWER KEEL FIRST TORSION
0.94	8-1	8-1	3-3	48-42	18-49	9-1	6-1	10. LOWER KEEL FIRST Y BENDING
0.97	11-2	11-3	11-6	3-3	14-76	34-2	16-10	11. KEEL TORSION AND BOOM BENDING
1.17	6-1	6-1	2-1	64-63	11-32	7-1	3-1	12. LOWER KEEL MODE - X DIR
1.29	21-2	18-2	9-14	5-10	28-68	14-2	6-2	13. TRANSVERSE BOOM MODE - Z DIR
1.40	11-2	13-2	1-2	4-3	14-82	49-2	8-7	14.TRANSVERSE BOOM MODE - X DIR
1.46	12-2	11-2	3-6	5-2	16-70	44-2	9-6	15. TRANSVERSE BOOM MODE - Z DIR
1.78	10-2	9-2	5-2	61-47	9-43	3-2	2-2	16. TRANSVERSE BOOM MODE -Y DIR
1.86	17-1	18-1	2-1	3-1	16-78	40-1	12-17	17. TRANSVERSE BOOM MODE - X DIR
1.91	17-1	17-1	20-22	3-23	13-47	5-1	5-5	18. TRANSVERSE BOOM/UPPER KEEL - Z DIR

Significant Modes in the Flight Path Direction

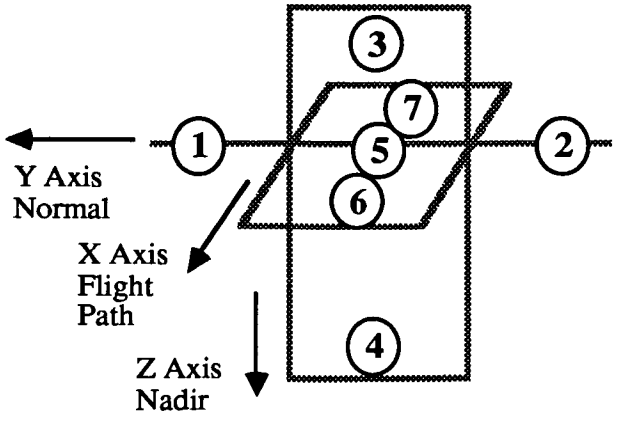

Table 4.2 Modal Strain and Kinetic Energy Participations

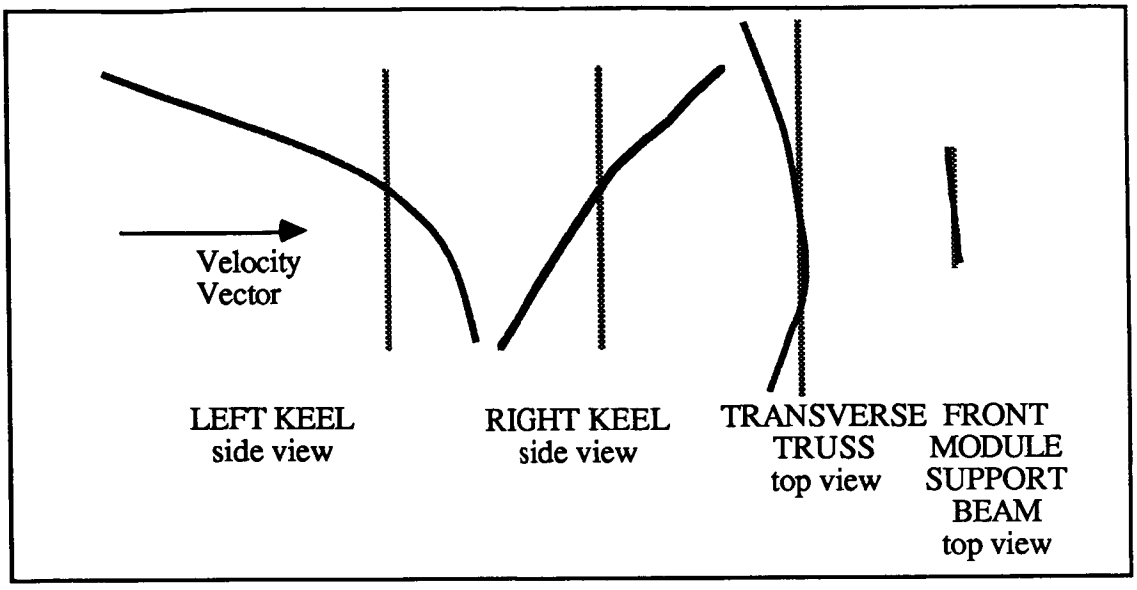

Figure 4.3 Mode-Shape deflections at 0.54 Hz

4.3 TRANSFER FUNCTIONS.

MSC/NASTRAN SOL 30 (modal frequency response solution) was used to compute the transfer functions at different points on the space station structure. By definition these are defined as the complex frequency response outputs due to unit input forces applied at the thruster locations. As stated earlier, the present study considers only the soft cycle harmonic inputs of the thrusters located at the top left and right keel locations (X=92.5m). A uniform modal damping coefficient of 0.5% was assumed in the present analysis and the transfer functions computed over the range of 0-2 Hz at different locations. The consequent acceleration amplitude/frequency plots at critical points are shown in Figures 4.4 through 4.9. The frequencies associated with the peak amplitudes identify the significant elastic modes. The points on the top keel are exicited by the 0.36 Hz and 0.54 Hz modes and the points on the bottom keel are excited by the 0.36 Hz, 0.54 Hz, 0.94 Hz and 1.17 Hz modes. Similarly the points at the module interfaces are exicited by 0.36 Hz, 1.4 Hz and 1.86 Hz modes.

4.4 DYNAMIC RESPONSE DUE TO THRUST PROFILE INPUTS

The number of harmonics and the harmonic frequencies for a specific thrust profile depend on the Cycle Period of the Thrust Profile. These can be computed using the Fourier series expressions discussed in the section 3.4. As mentioned above, the significant modes are exicited by the thrusters located on the top keel are 0.36 Hz and 0.54 Hz. The cycle periods chosen in the analysis are calculated by matching the thrust profile peak amplitude harmonic frequencies with the dominant structural frequencies. This selection procedure is based upon the following:

$$P_S = n_{PEAK} / f_S \qquad \text{4.1}$$

where:
P_S = Cycle Period
f_S = Structural Frequency in Hz.
n_{PEAK} = Harmonic corresponding to a peak Fourier Coefficient.

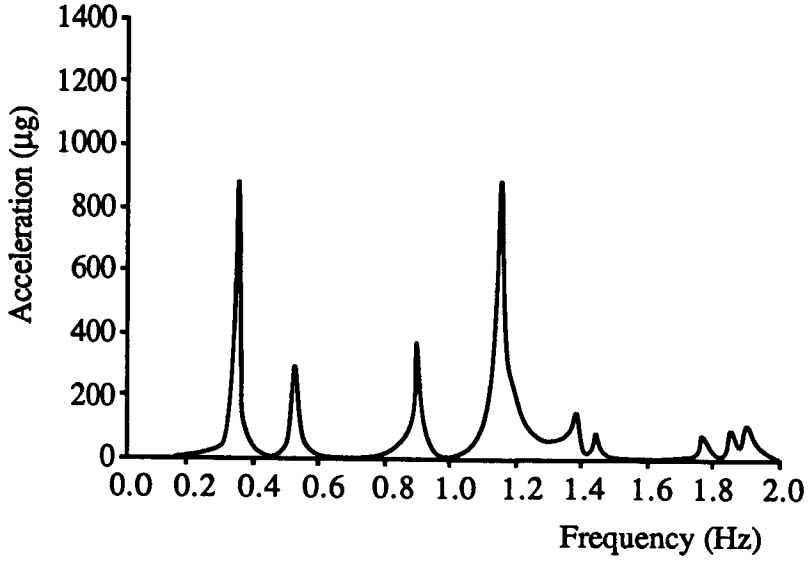

Figure 4.4 Bottom Keel (left) Transfer Function

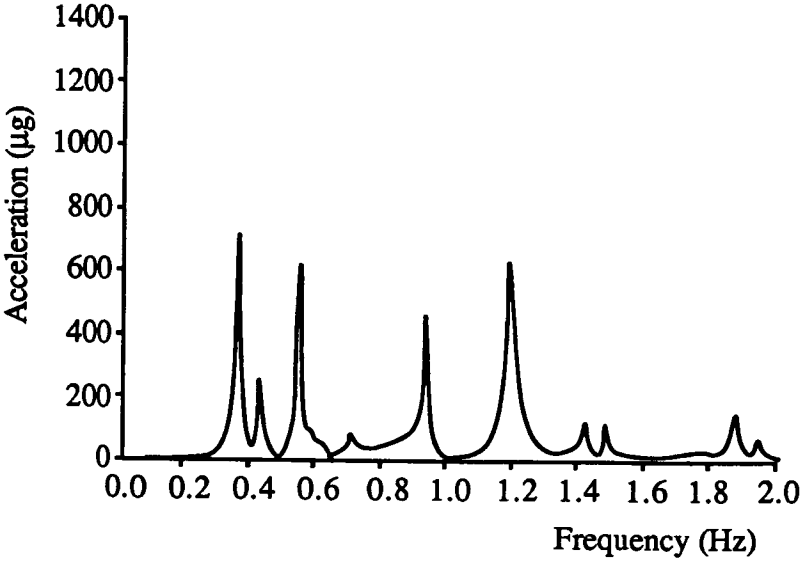

Figure 4.5 Botttom Keel (right) Transfer Function.

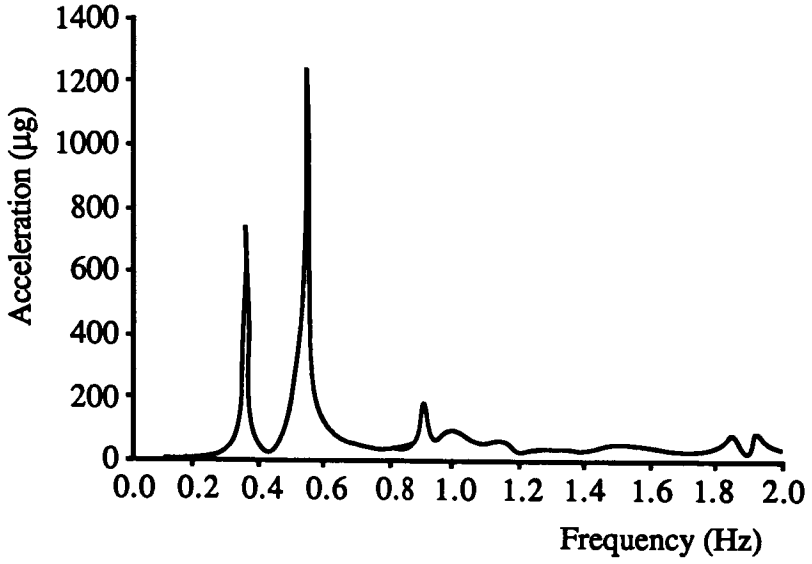

Figure 4.6 Top Keel (left) Transfer Function

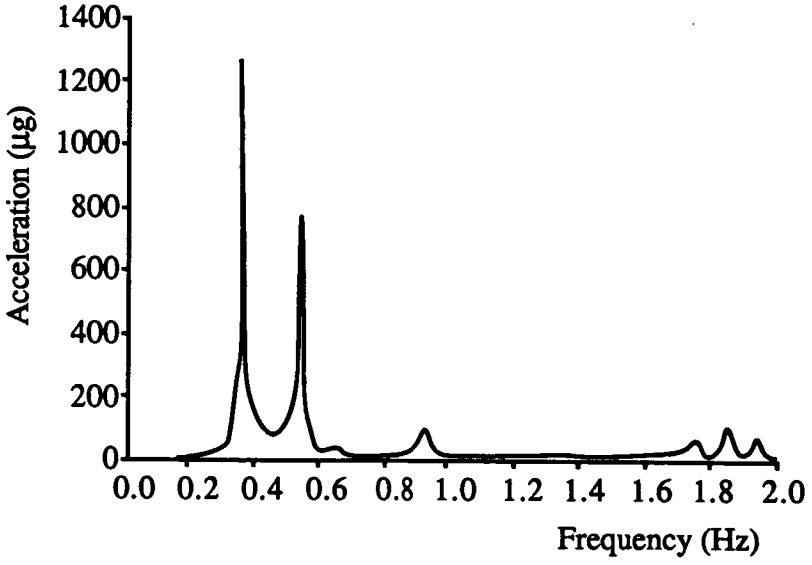

Figure 4.7 Top Keel (right) Transfer Function

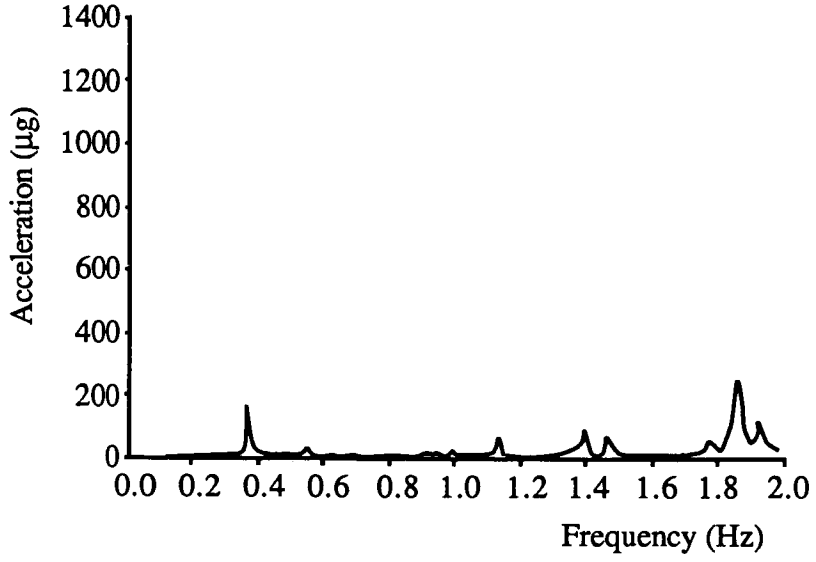

Figure 4.8 Module Interface with Central Transverse Boom Transfer Function

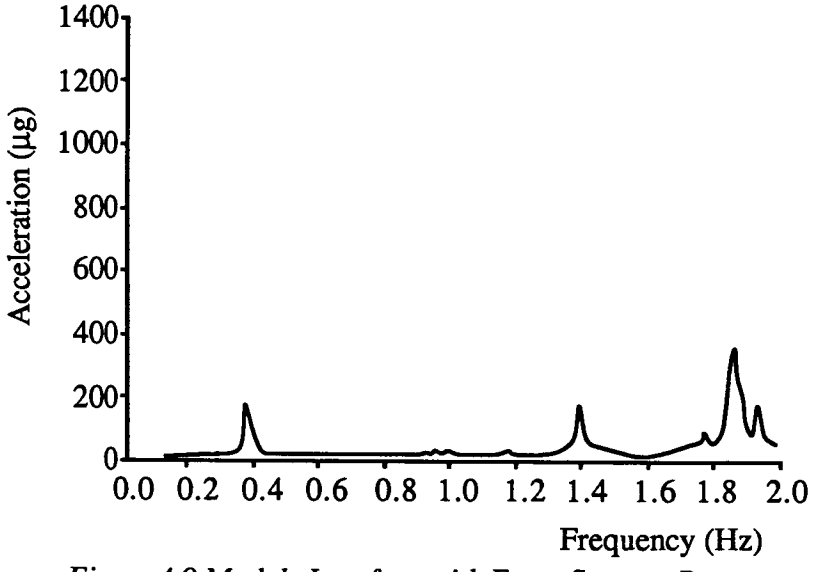

Figure 4.9 Module Interface with Front Support Beam Transfer Function

The harmonic response at the different points on the space station structure are computed using the following expression:

$$A(f_H) = H(f_H)^* F(f_H) \quad \text{____ 4.2}$$

where:

f_H	=	Harmonic Frequency
H	=	Transfer Function
F	=	Thrust Profile Harmonic Coefficient
A	=	Complex Harmonic Response

The maximum harmonic amplitude response versus period at a point on the keel and at the module interface point are shown in Figure 4.10.

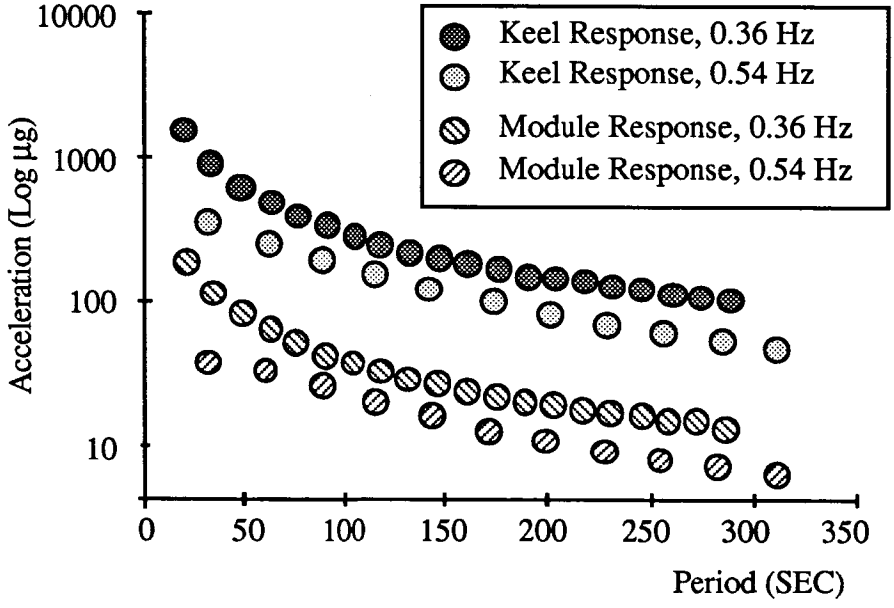

Figure 4.10 Frequency Response Amplitude vs Cycle period

The complex harmonic frequency response solutions are combined to yield the corresponding time response solutions using the expression

$$A(t) = \sum A_R(f_j).\cos(2\pi.f_j.t) + A_I(f_j).\sin(2\pi.f_j.t) \quad \text{____ 4.3}$$

where $A_R(f_H)$ and $A_I(f_H)$ are the real and imaginary components of the complex harmonic response.

The peak acceleration in the time domain are shown in Figure 4.11.

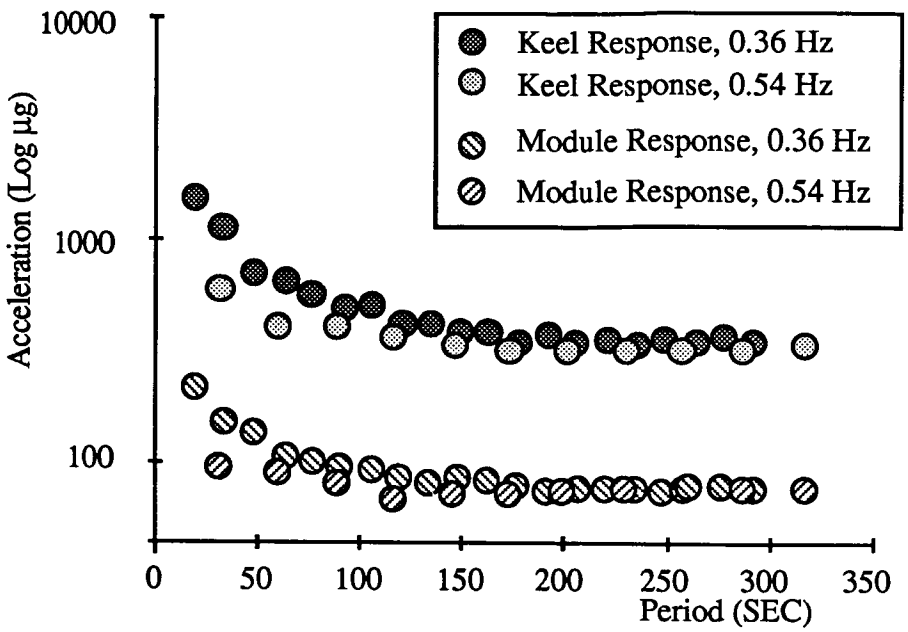

Figure 4.11 Time Response Maximum Amplitude vs Cycle period

4.5 INTERACTION ASSESSMENT.

From the results of the analysis presented in the previous section it can be seen that the lowest elastic mode frequency which contributed most to the response due to thrust profile harmonic inputs is 0.36 Hz. The other significant modal frequencies are 0.54, 0.94, 1.17, 1.4 and 1.86 Hz. The large number of harmonics associated with the large period thrust profiles excite a large number of structural modes. This can be seen from the relatively slow drop in the peak time response (Figure 4.11) compared to the peak amplitude response in the frequency domain (Figure 4.10). The flexible body response can be minimised by selecting thrust profile periods greater than about 30 times the period of the dominant elastic mode (0.36 Hz).

5.0 CONCLUSIONS

This paper has presented preliminary results from a study into the RCS/Structures interaction of the space station. The results indicate that a soft-limit cycle is an effective form of phase-plane logic; use of impulse is minimized and structural response can be restricted by choosing a suitably large attitude deadband.

Analysis of the frequency response and harmonic content of the thrust profiles suggest a continual reduction in flexible body response with increasing cycle perod. However, due to the increasing harmonic content with larger cycle periods, the reduction in response seen in the time domain actually plateaus. For periods greater than 30 times that of the fundamental mode the response was unchanged.

For the mode of control considered (uncoupled top keel thrusters) the resultant cycle period can be set at 100 seconds, effecting an attitude deadband of ±1 degree. The resultant flexible body peak accelerations are ±70μg at the modules and ±400μg at the top keel. This result was based upon the use of 50N thrusters; should larger thrusters be used then the accelerations would increase linearly.

Further analysis is required into the use of off-modulation of the bottom keel thrusters during reboost. Differing harmonic content ($\Delta P'$=80%) and frequency response should reduce the peak accelerations.

Acknowledgements

The authors would like to express their gratitude to R. Odbert for creating the structural dynamic model and his support throughout this study.

References

1. Marshall H. Kaplan, "Modern Spacecraft Dynamics & Control" pp.262.